An Alternative Approach to the Realization of Network Transfer Functions: The *N*-Path Filter

By L. E. FRANKS and I. W. SANDBERG

(Manuscript received April 14, 1960)

A particular time-varying network consisting of several parallel transmission paths, each containing input and output modulators, is described and analyzed. It is shown that, under certain conditions, the network may be characterized by a transfer function. A particular form of this transfer function yields periodic filtering characteristics over a limited frequency band without employing distributed elements. Techniques are also presented for realizing highly selective band-pass filters without the use of magnetic elements. Some practical applications are discussed in detail and experimental verification is presented.

I. INTRODUCTION

The application of conventional design techniques to network problems in systems operating at relatively low frequencies often leads to impractical circuits. In addition, designs based on active *RC* techniques are frequently very sensitive to small changes in element values. Alternatively, a time-varying network approach to the solution of a wide class of such problems appears to be particularly promising.

The time-varying network described and analyzed in this paper consists of a parallel combination of N identical linear time-invariant networks, each operating between input and output modulators. Attention is focused upon several properties of this configuration that are of theoretical as well as practical importance. In particular, these properties include:

i. Periodic filtering characteristics can be obtained over a limited frequency band without employing distributed elements. The practical uses for this property include the realization of low-frequency comb filters.

ii. Narrow-band band-pass and band-elimination filters can be realized at very low frequencies by networks free from magnetic elements. The center frequency of these filters is electronically controllable.

iii. An exact low-pass to band-pass translated version of the constituent network transfer function can be realized. The low-pass to band-pass transformation technique can also be applied to driving-point immittances.

The network under consideration is shown in block diagram form in Fig. 1. The time functions $u(t)$, $v(t)$, $x_n(t)$ and $y_n(t)$ may be interpreted to be either voltages or currents. The input modulators (multipliers) operate on the input $u(t)$ to produce the inputs

$$x_n(t) = u(t)p[t - (n - 1)\tau]$$

to the N identical linear time-invariant networks with impulse response $h(t)$. The outputs $y_n(t)$ are passed through output modulators to form path outputs $v_n(t)$. The final output $v(t)$ is the sum of the path outputs. The time functions $p[t - (n - 1)\tau]$ and $q[t - (n - 1)\tau]$ are periodic with period T, where $T = N\tau$.

In the next section the general input-output relationship for the N-path configuration is developed and discussed. The following sections are concerned with features associated with particular types of modulating functions. Some practical applications are discussed in detail and experimental verification is presented.

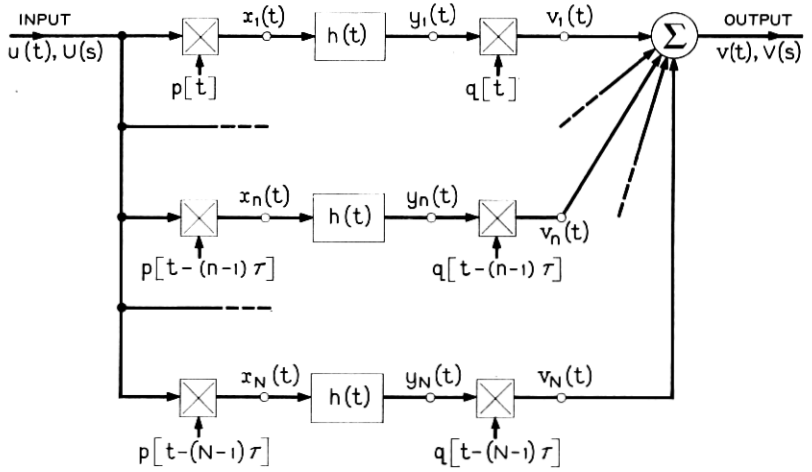

Fig. 1. — The N-path configuration.

II. GENERAL PROPERTIES OF THE N-PATH CONFIGURATION

2.1 *General Input-Output Relationship*

In this section we derive the relationship between $V(s)$ and $U(s)$, the network's frequency domain output and input.†

The periodic functions $p(t)$ and $q(t)$ can be expressed by their complex Fourier series:

$$\begin{aligned} p(t) &= \sum_{m=-\infty}^{m=+\infty} P_m e^{j\omega_0 mt}, \\ q(t) &= \sum_{l=-\infty}^{l=+\infty} Q_l e^{j\omega_0 lt}, \end{aligned} \tag{1}$$

where $\omega_0 = 2\pi/T = 2\pi/N\tau$. It is convenient to define

$$\begin{aligned} p_n(t) &= p[t - (n-1)\tau], \\ q_n(t) &= q[t - (n-1)\tau]. \end{aligned} \tag{2}$$

Since multiplication in the time domain corresponds to convolution in the frequency domain, it follows that

$$V(s) = \sum_{n=1}^{N} V_n(s) = \sum_{n=1}^{N} Y_n(s) \otimes Q_n(s). \tag{3}$$

Using the relation

$$J(s) \otimes \frac{1}{s-\alpha} = J(s-\alpha) \tag{4}$$

and (1), (2) and (3), we obtain

$$V(s) = \sum_{n=1}^{N} \sum_{l=-\infty}^{l=+\infty} Q_l e^{-j\omega_0(n-1)l\tau} X_n(s - jl\omega_0) H(s - jl\omega_0), \tag{5}$$

where

$$X_n(s)H(s) = Y_n(s). \tag{6}$$

Similarly,

$$X_n(s) = U(s) \otimes P_n(s) \tag{7}$$

and

$$X_n(s - jl\omega_0) = \sum_{m=-\infty}^{m=+\infty} P_m e^{-j\omega_0(n-1)m\tau} U[s - j(m+l)\omega_0].$$

† The time function and its Laplace transform are denoted, in accordance with the usual notation, by lower and upper case letters respectively.

Substituting (7) into (5) gives

$$V(s) = \sum_{n,l,m} Q_l P_m e^{-j\omega_0(n-1)(l+m)\tau} H(s - jl\omega_0) U[s - j(m + l)\omega_0]. \quad (8)$$

The summation over n is the following geometric series:

$$\sum_{n=1}^{N} e^{-j\omega_0(n-1)(l+m)\tau} \begin{cases} = N, & l + m = kN, \\ = 0, & \text{otherwise}, \end{cases} \quad (9)$$

where k is an integer. Using (9), we obtain

$$V(s) = N \sum_{k,l} Q_l P_{kN-l} H(s - jl\omega_0) U(s - jkN\omega_0). \quad (10)$$

It is convenient to write (10) in the form

$$V(s) = \sum_{k=-\infty}^{k=+\infty} F(k,s) U(s - jkN\omega_0), \quad (11)$$

$$F(k,s) = N \sum_{l=-\infty}^{l=+\infty} Q_l P_{kN-l} H(s - jl\omega_0). \quad (12)$$

Expressions (11) and (12) constitute the general input-output relationship for the N-path structure.

2.2 *Transfer Function for N-Path Configuration*

The quantity $F(k,s)$ in (11) and (12) completely characterizes the time-varying network of Fig. 1. It describes operationally the relation between the input signal and output signal, as is shown symbolically in Fig. 2(a). In this sense, $F(k,s)$ may be considered analogous to the characterization of a constant-parameter network in terms of a transfer function. A feature of the N-path configuration of particular interest from the network theory viewpoint is that, with certain band-limiting restrictions on the input and output signals, a transfer function relation between input and output can be derived. It is this property that will be investigated in the remainder of the paper.

If $U(s)$ evaluated on the $j\omega$-axis essentially vanishes outside the interval $|\omega| < N\omega_0/2$, it follows that

$$V(j\omega) = F(0,j\omega) U(j\omega) \qquad \text{in } |\omega| < \frac{N\omega_0}{2}. \quad (13)$$

Furthermore, if $V(j\omega)$ vanishes outside the interval $|\omega| < N\omega_0/2$, then $V(s)$ and $U(s)$ can be related by a transfer function $T(s)$:

$$T(s) = \frac{V(s)}{U(s)},$$

where

$$\begin{aligned} T(j\omega) &= F(0,j\omega) \qquad \text{in } |\omega| < \frac{N\omega_0}{2}, \\ &= 0 \qquad\qquad \text{in } |\omega| > \frac{N\omega_0}{2}. \end{aligned} \tag{14}$$

These band-limiting constraints can be accomplished by preceding and following the time-varying network with ideal low-pass filters having cutoff at $\omega_c = N\omega_0/2$. With the addition of these low-pass filters, the time-varying network is equivalent to a constant-parameter network having a transfer function, $F(0,s)$, preceded and followed by ideal low-pass filters, as shown in Fig. 2(b).

An alternate expression for the transfer function will be developed in the following equations. This expression leads to a closed form for $F(0,s)$.

From (12),

$$F(0,s) = N \sum_{l=-\infty}^{\infty} P_{-l} Q_l H(s - jl\omega_0). \tag{15}$$

This can be written as the Laplace transform of the product of the im-

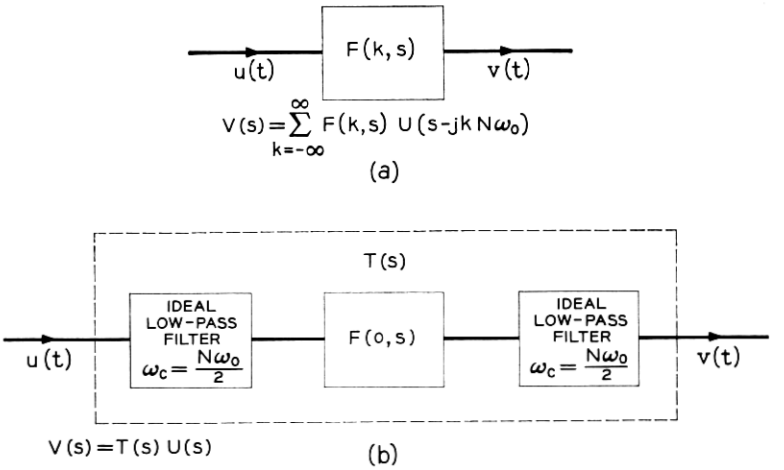

Fig. 2 — (a) Symbolic representation of $F(k,s)$; (b) equivalent constant-parameter network.

pulse response of the component networks, $h(t)$, and a periodic function with period T:

$$\begin{aligned} F(0,s) &= \mathcal{L}\left[h(t)N\sum_{l=-\infty}^{\infty} P_{-l}Q_l e^{+jl\omega_0 t}\right] \\ &= \mathcal{L}\left[h(t)\sum_{k=-\infty}^{\infty} r(t-kT)\right], \end{aligned} \tag{16}$$

where

$$\sum_{k=-\infty}^{\infty} r(t-kT) = N\sum_{l=-\infty}^{\infty} P_{-l}Q_l e^{+jl\omega_0 t}. \tag{17}$$

The pulse $r(t)$ depends only on the modulating functions and not on the response characteristics of the component networks. The identification of $r(t)$ with $p(t)$ and $q(t)$ is not unique. However, a particularly useful relation is obtained by considering $p(t)$ and $q(t)$ to be represented by infinite pulse trains wherein each pulse assumes the shape of one period of the modulating functions; that is,

$$\begin{aligned} p(t) &= \sum_{k=-\infty}^{\infty} a(t-kT), \\ q(t) &= \sum_{k=-\infty}^{\infty} b(t-kT), \end{aligned} \tag{18}$$

where

$$\begin{aligned} a(t) &= p(t) \qquad \text{in } 0 \leqq t \leqq T, \\ &= 0 \qquad \text{otherwise;} \\ b(t) &= q(t) \qquad \text{in } 0 \leqq t \leqq T, \\ &= 0 \qquad \text{otherwise.} \end{aligned} \tag{19}$$

Then it can be shown that

$$r(t) = \frac{N}{T}\int_0^T a(y)b(y+t)\,dy \tag{20}$$

satisfies (17). Notice that $r(t)$, like $a(t)$ and $b(t)$, is a duration-limited function, in that

$$r(t) = 0 \qquad \text{for } |t| \geqq T. \tag{21}$$

Since the Laplace transform of a product of time functions is given by

the convolution of their transforms, (16) becomes

$$F(0,s) = H(s) \otimes \mathfrak{L}\left[\sum_{k=-\infty}^{\infty} r(t - kT)\right] \tag{22}$$

and

$$\mathfrak{L}\left[\sum_{k=-\infty}^{\infty} r(t - kT)\right] = R(s) + \frac{N}{T}\sum_{k=1}^{\infty} A(-s)B(s)e^{-skT}, \tag{23}$$

where

$$\begin{aligned} R(s) &= \int_0^T r(t)e^{-st}\,dt, \\ A(s) &= \int_0^T a(t)e^{-st}\,dt, \\ B(s) &= \int_0^T b(t)e^{-st}\,dt. \end{aligned} \tag{24}$$

The terms in k form a geometric series that is readily summed, so that

$$F(0,s) = H(s) \otimes \left[R(s) + \frac{\frac{N}{T}A(-s)B(s)e^{-sT}}{1 - e^{-sT}}\right]. \tag{25}$$

2.3 *Transfer Function for Rational $H(s)$*

If we now assume that $H(s)$ is rational in s and regular at infinity, then, assuming only simple poles,

$$H(s) = c_0 + \sum_{i=1}^{M} \frac{c_i}{s - s_i}. \tag{26}$$

From (25),

$$F(0,s) = c_0 r(0) + \sum_{i=1}^{M} c_i \left[R(s - s_i) + \frac{\frac{N}{T}A(s_i - s)B(s - s_i)e^{-(s-s_i)T}}{1 - e^{-(s-s_i)T}}\right]. \tag{27}$$

The functions $R(s)$ and $A(-s)B(s)$ have no singularities in the finite part of the s-plane. Thus, the singularities of $F(0,s)$ are given by the zeros of $1 - e^{-(s-s_i)T}$, which lie equally spaced at intervals of $2\pi/T$ on lines parallel to the $j = \omega$ axis.

III. SPECIFIC TYPES OF MODULATING FUNCTIONS

In this section the properties of the N-path configuration are examined for specific types of modulation that reveal particularly interesting properties of the structure.

3.1 *Sinusoidal Modulation*

Suppose that the modulating functions possess only a finite number of sinusoidal components:

$$\begin{aligned} p(t) &= \sum_{m=-M}^{M} P_m e^{jm\omega_0 t}, \\ q(t) &= \sum_{m=-M}^{M} Q_m e^{jm\omega_0 t}, \end{aligned} \tag{28}$$

where

$$P_{-m} = P_m^* \qquad \text{and} \qquad Q_{-m} = Q_m^*.$$

The case for $N > 2M$ deserves special attention, for then

$$Q_l P_{kN-l} = 0 \qquad \text{for } k \neq 0,$$

and, from (11) and (12),

$$\frac{V(s)}{U(s)} = F(0,s). \tag{29}$$

Therefore, the network exhibits a transfer function $T(s)$ for $N > 2M$, without band-limiting restrictions, which is given by

$$T(s) = F(0,s).$$

Note that the transfer function is a finite sum of frequency-translated versions of $H(s)$. In particular, when $P_m, Q_m = 0$ for $|m| \neq 1$, we have

$$T(s) = N[a_1 H(s - j\omega_0) + a_1^* H(s + j\omega_0)], \tag{30}$$

where

$$a_1 = Q_1 P_{-1},$$

a "low-pass to band-pass transformation" of the transfer function $H(s)$†.

† This result can also be obtained with only two parallel paths.[1] Single sinusoid modulating functions are employed, the two functions in one path being in phase with each other and in quadrature with the functions in the other path. A similar configuration has been considered by Hines and Desoer in unpublished work.

A particularly difficult practical network problem is the low-frequency realization of highly selective band-pass filters. Procedures that avoid the use of magnetic elements are inviting, but active RC techniques often lead to a high degree of transfer function sensitivity to both the active and passive parameters. An alternate approach based on (30) appears to be attractive, and should provide a considerable increase in the degree of immunity from network parameter variations. Implementation of a similar approach is discussed in more detail in Section 5.2.

The transfer function poles of a passive RC network are distinct and on the negative-real axis of the complex-frequency plane. Consequently, if $H(s)$ is the transfer function of an RC network, the over-all transfer function $T(s)$ of (30) can have only distinct pairs of complex-conjugate poles with identical imaginary parts. It is desirable to circumvent this restriction without employing magnetic or active elements. It is sufficient to consider the synthesis of the transfer function

$$T(s) = \frac{N(s)}{D(s)}, \tag{31}$$

where $T(s)$ has only simple complex-conjugate poles, since transfer functions with multiple-order poles can be realized as the product of transfer functions having only simple poles. We assume that $T(s)$ is stable and regular at infinity. Equation (31) can be expressed as

$$T(s) = K_\infty + \sum_{i=1}^{M} \frac{b_i}{s + \sigma_i - j\omega_i} + \frac{b_i^*}{s + \sigma_i + j\omega_i}. \tag{32}$$

From (30), each of the series terms can be separately realized with the passive transfer function $H_i(s) = 1/(s + \sigma_i)$. Evidently we require

$$b_i = NQ_{1i}P_{-1i}. \tag{33}$$

Hence, a realization of (32) consists of M similar sections in parallel, with an additional section that realizes the constant term. The main objection to this realization technique is that a large number of modulators may be required, but it demonstrates that any transfer function that is regular at infinity and stable can be realized with sinusoidal modulators, a source of modulating frequencies and simple passive RC structures.

While this paper is primarily concerned with the synthesis of transfer functions, it is worthwhile to sacrifice some degree of continuity here to point out the relevance and extension of the preceding discussion to the synthesis of driving-point impedances. The results of this section apply also to the case where $U(s)$ and $V(s)$ are interpreted to correspond to

the transforms of voltage and current at the same port. The forms taken by the network for this special application are shown in Fig. 3. Suppose, for example, that the nth two-port network in Fig. 3(a) is characterized by

$$\begin{aligned} i_n'(t) &= p[t - (n-1)\tau]e_n(t), \\ i_n(t) &= q[t - (n-1)\tau]e_n'(t), \end{aligned} \tag{34}$$

where $p(t)$ and $q(t)$ are given by (28). The driving-point admittance

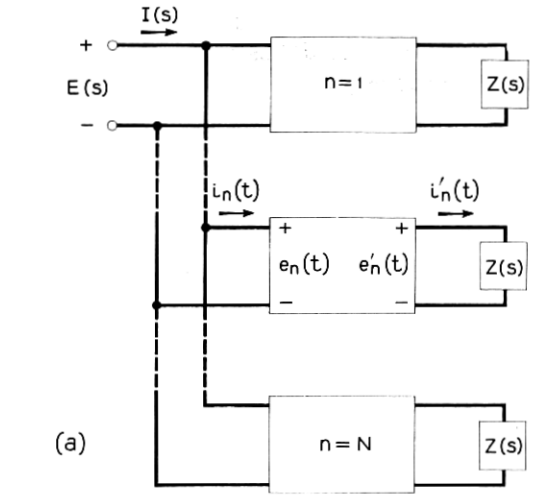

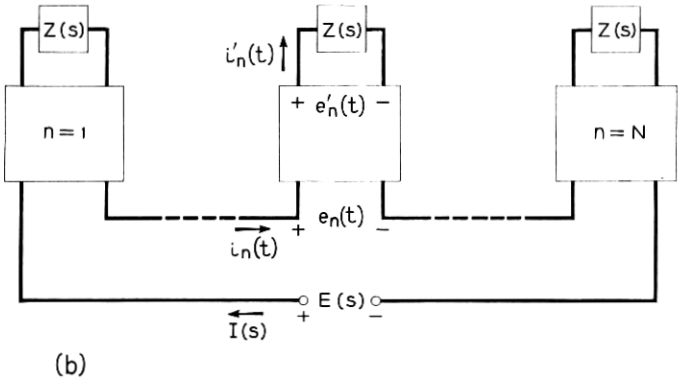

Fig. 3 — Forms taken by network when $U(s)$ and $V(s)$ are interpreted as corresponding to transforms of voltage and current at same port.

$Y_{in} = I(s)/E(s)$ is given by $F(0,s)$, with $H(s)$ replaced by $Z(s)$. That is,

$$Y_{in}(s) = NP_0Q_0Z(s) + N\sum_{m=1}^{M}[a_mZ(s - jm\omega_0) + a_m^*Z(s + jm\omega_0)], \tag{35}$$

where

$$a_m = Q_mP_{-m} \quad \text{and} \quad N > 2M.$$

For the special case where P_m, $Q_m = 0$ for $|m| \neq 1$ and a_1 is real,

$$Y_{in}(s) = Na_1[Z(s - j\omega_0) + Z(s + j\omega_0)]. \tag{36}$$

For example, if $Z(s) = 1/sC$,

$$Y_{in}(s) = \frac{2Na_1}{C}\frac{s}{s^2 + \omega_0^2}, \tag{37}$$

the admittance of an inductor and capacitor in series.

As in the transfer function case, (36) (and the analogous relations for the following three other networks discussed here) can be realized with only two parallel paths. Single sinusoid modulating functions are employed, the two functions in each two-port network being in quadrature with the corresponding functions in the other two-port network.

If the two-port networks in Fig. 3(a) are characterized by

$$\begin{aligned} e_n'(t) &= p[t - (n - 1)\tau]e_n(t), \\ i_n(t) &= q[t - (n - 1)\tau]i_n'(t), \end{aligned} \tag{38}$$

we obtain

$$Y_{in}(s) = NP_0Q_0Y(s) + N\sum_{m=1}^{M}[a_mY(s - jm\omega_0) + a_m^*Y(s + jm\omega_0)], \tag{39}$$

where

$$Y(s) = \frac{1}{Z(s)}.$$

The two dual networks take the form shown in Fig. 3(b).

3.2 *Jump Modulation*

The physical implementation of the transfer function of (15) can be accomplished without the difficulties normally encountered in the realiza-

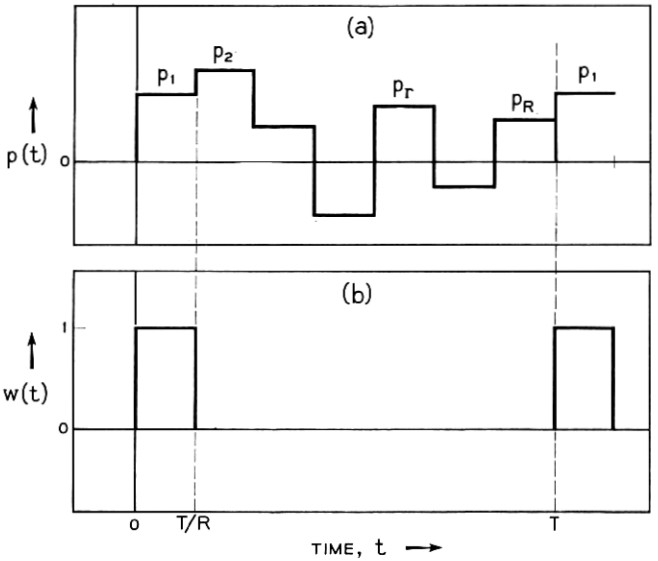

Fig. 4 — (a) Modulating function $p(t)$ with R jumps in fundamental interval T; (b) periodic switching function $w(t)$.

tion of accurate multiplier circuitry by means of a scheme called *jump modulation*. This scheme uses modulating functions having a finite number of equally spaced discontinuities or jumps in each fundamental interval. The functions assume a constant value between jumps. Modulators of this type can be realized by conventional switching techniques. Suppose that the modulating function $p(t)$ has R jumps in the fundamental interval T, as shown in Fig. 4(a):

$$p(t) = \sum_{r=1}^{R} p_r w\left[t - (r-1)\frac{T}{R}\right] = \sum_{m=-\infty}^{\infty} P_m e^{j(m2\pi/T)t} \qquad (40)$$

where $w(t)$ is the periodic switching function shown in Fig. 4(b).

The Fourier coefficients of $p(t)$ are given by

$$P_m = \frac{1}{T}\int_0^T p(t)\, e^{-j(m2\pi/T)t}\, dt = \frac{1}{T}\sum_{r=1}^{R} p_r \int_{(r-1)(T/R)}^{r(T/R)} e^{-j(m2\pi/T)}\, dt. \qquad (41)$$

Thus, the sequence of values P_m is given by a linear transformation of the sequence of values, p_r :

$$P_m = \sum_{r=1}^{R} \frac{e^{j(m\pi/R)} \sin\dfrac{m\pi}{R}}{m\pi} e^{-j(2\pi/R)mr} p_r\,. \qquad (42)$$

For design purposes, the inverse of this transformation is desired in order that an appropriate set, p_r, can be determined from an arbitrarily prescribed set, P_m. Obviously, only R values can be independently prescribed for the complex numbers P_m and, since $p(t)$ is real, it is always required that $P_{-m} = P_m^*$ and P_0 be real. Hence, for example, a set of values p_r can be found such that all the Fourier coefficients P_m can be arbitrarily specified for $|m| \leqq R/2$. In this case, the inverse transformation corresponding to (42) is relatively simple:†

$$p_r \ (R \text{ odd}) = \sum_{m=-(R-1)/2}^{(R-1)/2} \frac{e^{-j(m\pi/R)} \dfrac{m\pi}{R}}{\sin \dfrac{m\pi}{R}} e^{j(2\pi/R)rm} P_m . \tag{43}$$

When R is even,‡

$$p_r \ (R \text{ even}) = \sum_{m=-R/2+1}^{R/2-1} \frac{e^{-j(m\pi/R)} \dfrac{m\pi}{R}}{\sin \dfrac{m\pi}{R}} e^{j(2\pi/R)rm} P_m - j \frac{\pi}{2} (-1)^r P_{R/2} . \tag{44}$$

A case of particular interest in the N-path configuration is for $R = N$, when the jumps occur simultaneously in all paths and a common timing source can be used for operating the switches. If the bandwidth of the component networks is sufficiently small compared to ω_0, the transfer function can be expressed approximately in terms of the first $N/2$ Fourier coefficients:

$$T(j\omega) \cong N \sum_{m=-N/2}^{N/2} Q_m P_{-m} H(j\omega - jm\omega_0), \tag{45}$$

where all the values of either P_m or Q_m or both can be arbitrarily chosen.

3.3 *Pulse Modulation*

A special case of jump modulation of considerable practical importance is for the set $\{p_1 = 1, p_2 = p_3 = \cdots = p_{R_1} = 0\}$ and $\{q_1 = 1, q_2 = q_3 = \cdots = q_{R_2} = 0\}$, so that

† See Appendix A for derivation of the inverse transformation.

‡ From (42), it is seen that the real part of $P_{R/2}$ must vanish, since

$$P_{R/2} = e^{j(\pi/2)} \frac{\sin (\pi/2)}{R(\pi/2)} \sum_{r=1}^{R} (-1)^r p_r .$$

$$\begin{aligned} p(t) &= w_1(t), \\ q(t) &= w_2(t), \end{aligned} \tag{46}$$

If the input generator, $u(t)$, is a current source, each modulator in Fig. 1 can be replaced by a simple switch. In fact, when R_1 and $R_2 > N$, the entire set of input and output modulators would then be equivalent to a pair of N-contact rotary switches on a common shaft rotating at a rate of $1/T$ cps. The dwell time at each contact of the input and output switches is given by $d_1 = T/R_1$ and $d_2 = T/R_2$, respectively. In this case, the switches are essentially signal-sampling devices, hence the general configuration using this type of modulation will hereafter be referred to as the *N-path sampled-data network*.

Besides being relatively simple to implement, the N-path sampled-data network has some very interesting transfer function characteristics. If the component networks have a low-pass characteristic with bandwidth small compared to ω_0, the transfer function for large N will appear as a sequence of narrow, equally spaced passbands of identical shape and nearly equal height, centered at integral multiples of ω_0. This corresponds to the so-called "comb filter" characteristic, which is frequently employed in the detection of periodic signals immersed in wide band noise. Furthermore, it will be shown that the function $F(0,s)$ becomes periodic on the $j\omega$-axis as the dwell times d_1 and d_2 approach zero. When $H(s)$ is rational in s, this periodic function is of the form generally associated with the network functions of circuits containing resistors and ideal delay lines.

IV. TRANSFER FUNCTION FOR N-PATH SAMPLED-DATA NETWORK

The expression for $F(0,s)$ in terms of $r(t)$ as given in (22) is especially convenient for finding the transfer function of the N-path sampled-data network. Also, if $H(s)$ is rational in s and regular at infinity, then (27) gives an exact closed-form expression for $F(0,s)$.

Suppose, for example, that $d_1 = d_2 = d < T$. Then $r(t)$ is simply the triangular pulse,

$$\begin{aligned} r(t) &= \frac{N}{T}(d - |t|) \qquad \text{in } |t| \leqq d, \\ &= 0 \qquad\qquad\quad \text{otherwise}, \end{aligned} \tag{47}$$

so

$$R(s) = \frac{N}{T}\left[\frac{ds - (1 - e^{-sd})}{s^2}\right] \tag{48}$$

and

$$\begin{aligned} A(-s)B(s) &= \frac{(1 - e^{sd})}{-s} \frac{(1 - e^{-sd})}{s} \\ &= \frac{e^{sd} - 2 + e^{-sd}}{s^2} . \end{aligned} \tag{49}$$

Then, assuming $H(s)$ to be in the form of (26), the transfer function is obtained directly from (27):

$$F(0,s) = \frac{c_0 Nd}{T} + \frac{N}{T} \sum_{i=1}^{M} \left(\frac{c_i}{\lambda_i^2}\right) \frac{(e^{-\lambda_i d} - 1 + \lambda_i d) + (e^{\lambda_i d} - 1 - \lambda_i d) e^{-\lambda_i T}}{1 - e^{-\lambda_i T}} , \tag{50}$$

where

$$\lambda_i = s - s_i .$$

When $| \lambda_i d | \ll 1$, the transfer function can be approximated by a function that is periodic for values of s on any line parallel to the $j\omega$-axis. If the first three terms in the power series expansion for $e^{\lambda_i d}$ and $e^{-\lambda_i d}$ are retained, then

$$F(0,s) \cong \frac{c_0 Nd}{T} + \frac{Nd^2}{2T} \sum_{i=1}^{M} c_i \frac{1 + e^{-(s-s_i)T}}{1 - e^{-(s-s_i)T}} \tag{51}$$

for

$$| s - s_i | d \ll 1.$$

The relation (51) can be obtained in a different manner by application of conventional sampled-data techniques.[2] These techniques provide an alternate approach worthy of investigation, since they lead to a simple single-path sampled-data network, which is equivalent to the N-path sampled-data network. The approximation involved in this method of analysis consists of replacing sampling switches by impulse modulators (IM), as shown in Fig. 5(a). The train of narrow rectangular modulating pulses, $w(t)$, has been replaced by an impulse train, where the magnitude of each impulse is equal to the area of the corresponding rectangular pulse. Hence,

$$p(t) \cong d_1 \sum_{k=-\infty}^{\infty} \delta(t - kT), \tag{52}$$

$$q(t) \cong d_2 \sum_{k=-\infty}^{\infty} \delta(t - kT). \tag{53}$$

Then,

$$P_m = \frac{d_1}{T} \qquad \text{for all } m$$

and

$$Q_m = \frac{d_2}{T} \qquad \text{for all } m.$$

In this case, $F(k,s)$ in (12) is independent of k and

$$F(k,s) = G(s) = N \frac{d_1 d_2}{T^2} \sum_{l=-\infty}^{\infty} H(s - jl\omega_0). \tag{54}$$

Then,

$$V(s) = G(s) \left[\sum_{m=-\infty}^{\infty} U(s - jkN\omega_0) \right]. \tag{55}$$

This input-output relation is identical to that of a single-path sampled-data network having an input impulse modulator with sampling interval, $\tau = T/N$, followed by a network with a transfer function, $\tau G(s)$, which, when $s = j\omega$, is periodic with period ω_0. The periodic property of the

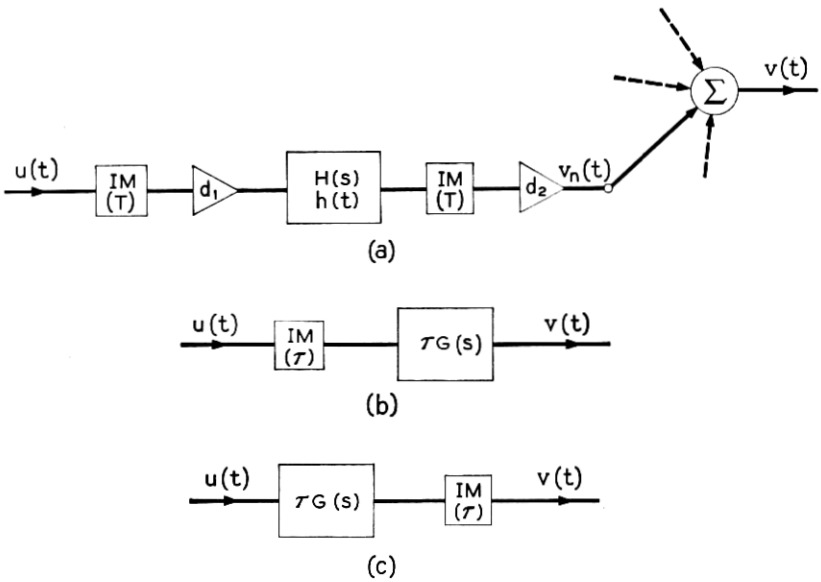

Fig. 5 — (a) Approximate representation of N-path sampled-data network; (b) and (c) equivalent single-path networks.

network following the impulse modulator in Fig. 5(b) allows the derivation of another equivalent network with the impulse modulator at the output, as shown in Fig. 5(c). These simple equivalent networks are very convenient for analysis purposes when one or more N-path configurations are component parts of a larger system.

The Fourier coefficients for the expression of $G(s)$ when $s = j\omega$ are obtained directly from the sample values, $h(rT)$, of the impulse response of one of the component networks. If

$$G(j\omega) = \sum_{r=-\infty}^{\infty} g_r \, e^{jr(2\pi\omega/\omega_0)},$$

then

$$\begin{aligned} g_r &= \frac{1}{\omega_0} \int_{-\omega_0/2}^{\omega_0/2} G(j\omega) \, e^{-j(r2\pi\omega/\omega_0)} \, d\omega \\ &= \left(\frac{Nd_1d_2}{T^2}\right) \frac{1}{\omega_0} \int_{-\omega_0/2}^{\omega_0/2} \sum_{l=-\infty}^{\infty} H(j\omega - jl\omega_0) \, e^{-j(r2\pi\omega/\omega_0)} \, d\omega \\ &= \left(\frac{Nd_1d_2}{T^2}\right) (T) \left[\frac{1}{2\pi} \int_{-\infty}^{\infty} H(j\omega) \, e^{-jrT\omega} \, d\omega\right], \end{aligned} \tag{56}$$

$$g_r = \frac{Nd_1d_2}{T} h(-rT). \tag{57}$$

The integral in (56) is the Fourier inversion integral for $h(t)$. At discontinuities in $h(t)$ the inversion integral gives the mean value of the right- and left-hand limits at the discontinuity. Hence, for physically realizable component networks.

$$G(s) = \frac{Nd_1d_2}{T} \left[\frac{h(0+)}{2} + \sum_{r=1}^{\infty} h(rT) \, e^{-rsT}\right]. \tag{58}$$

This expansion is particularly useful when $H(s)$ is a rational function of s. In this case, the series can be summed and $G(s)$ is given in closed form. Assuming $H(s)$ has simple poles, then†

$$h(t) = \sum_{i=1}^{M} c_i \, e^{s_i t} \qquad \text{for} \quad t \geqq 0 \tag{59}$$

and, from (58),

$$G(s) = \frac{Nd_1d_2}{T} \sum_{i=1}^{M} c_i \left(\frac{1}{2} + \sum_{r=1}^{\infty} e^{r(s_i - s)T}\right). \tag{60}$$

† In this analysis we require that $H(s) \to 0$ as $s \to \infty$ ($c_0 = 0$) since the Laplace transform for a product of impulse functions is not defined.

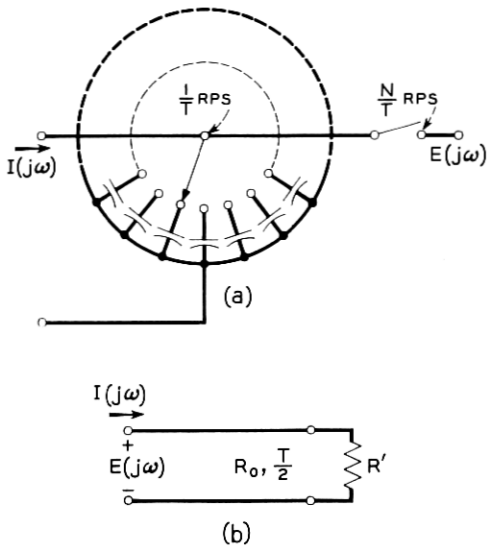

Fig. 6 — The N-capacitor element.

The sum over r in (60) is a geometric series and can be written in closed form, so that

$$G(s) = \frac{Nd_1d_2}{2T} \sum_{i=1}^{M} c_i \frac{1 + e^{(s_i - s)T}}{1 - e^{(s_i - s)T}}. \tag{61}$$

Note the equivalence between (61) obtained by conventional sampled-data techniques and the direct approximation of (51) to the transfer function of the N-path sampled-data network.

A simple example that illustrates the application of the preceding techniques is the case where each component network is a single capacitor, as shown in Fig. 6(a).† Capacitor loss is accounted for by the inclusion of a resistance, R_c, across each capacitor. The relation between input current and output voltage is represented by $G(s)$ in (61), where

$$H(s) = \frac{\frac{1}{C}}{s + \frac{1}{R_cC}}, \tag{62}$$

† This case has been described in the literature.[3,4]

so that

$$\begin{aligned} M &= 1, \\ s_1 &= -\frac{1}{R_c C}, \\ c_1 &= \frac{1}{C}, \\ d_1 &= d_2 = d \end{aligned} \tag{63}$$

and

$$G(s) = R_0 \left[\frac{1 + \rho e^{-sT}}{1 - \rho e^{-sT}} \right], \tag{64}$$

where

$$\rho = e^{-T/R_c C}$$

and

$$R_0 = \frac{Nd^2}{2TC}.$$

The expression of (64) is equal to the driving-point impedance of a length of lossless transmission line of characteristic impedance, R_0, terminated at a distance corresponding to an electrical delay of $T/2$ seconds. The termination is characterized by a reflection coefficient $\rho = e^{-T/R_c C}$, or equivalently, by a resistance, R', where

$$R' = R_0 \left(\frac{1 + \rho}{1 - \rho} \right). \tag{65}$$

If the capacitors are lossless, then

$$G(s) = \frac{Nd^2}{2TC} \left(\frac{1 + e^{-sT}}{1 - e^{-sT}} \right) = R_0 \coth \frac{sT}{2}, \tag{66}$$

which is equal to the driving-point impedance of the same length of lossless transmission line with open-circuit termination.

V. SOME PRACTICAL APPLICATIONS FOR THE N-PATH SAMPLED-DATA NETWORK

5.1 *Delay Network*

The transcendental nature of $G(s)$ of (66) for the N-capacitor element suggests the possibility of realizing an all-pass constant-delay characteris-

tic over a limited bandwidth without the use of inductors. One of several possible configurations for accomplishing this is the simple feedback network shown in Fig. 7, where the N-capacitor element is contained in the feedback path.

For the analysis of this circuit, it is assumed that the forward gain, μ, is sufficiently large that the error voltage, $v_1 + v_3$, is essentially zero. Note that

$$v_2(t) = v_3(t) + R_2 i(t) \tag{67}$$

and, hence, because of the low-pass filter at the output, only the components of $V_3(j\omega)$ and $I(j\omega)$ in the frequency range $|\omega| \leqq N\omega_0/2$ are of interest. If $V_1(j\omega)$ [and hence $V_3(j\omega)$] is limited to this same bandwidth, then

$$I(s) = Y(s)V_3(s)$$

and

$$\frac{V_4}{V_1}(s) = -[1 + R_2 Y(s)] + K \tag{68}$$

over the frequency band of interest, and $Y(s)$ is a function of the N-path type.

The constant-delay characteristic is obtained by making the R_1C time constant very small compared to the contact dwell time, d. Roughly speaking, this means that the capacitors charge up to the applied voltage in the time interval d, during which their respective switches are closed, and the resulting current flow is a sequence of narrow exponentially decaying pulses occurring τ seconds apart. An approximate representation

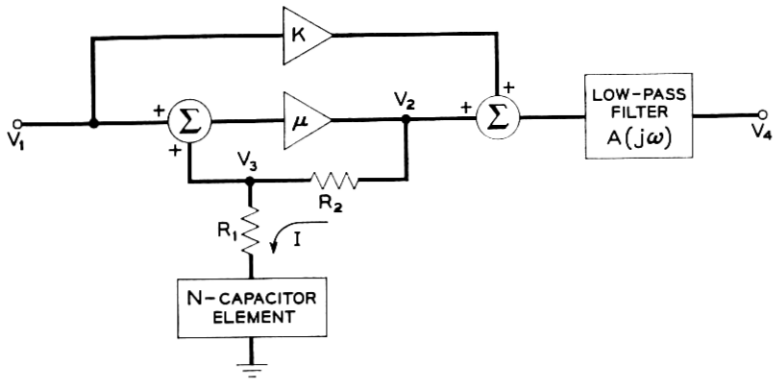

Fig. 7 — Constant-delay network.

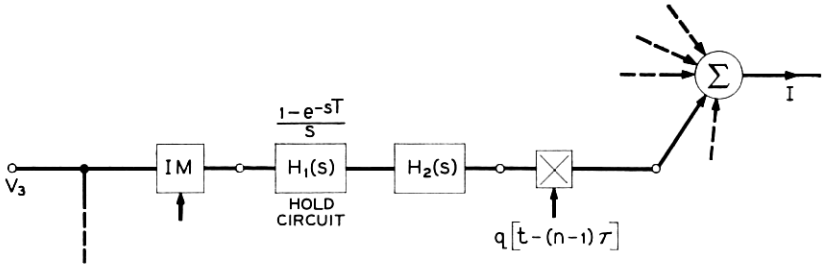

Fig. 8 — N-path network used for describing the behavior of the constant-delay network.

of this behavior in terms of the general N-path configuration is shown in Fig. 8. The applied voltage, V_3, is sampled with an impulse modulator at the time of the nth switch closure and held at this value for T seconds by means of the hold circuit, $H_1(s)$. The current flowing in the series combination of R_1 and C in response to the applied voltage steps is obtained by means of the transfer function

$$H_2(s) = \frac{1}{R_1} \frac{s}{s + \alpha}, \tag{69}$$

where

$$\alpha = \frac{1}{R_1 C} \gg d.$$

The transfer function $Y(s)$ is obtained from (25), where

$$\begin{aligned} A(s) &= 1, \\ R(s) &= \frac{N}{T} B(s) = \frac{N}{T}\left(\frac{1 - e^{-sd}}{s}\right). \end{aligned} \tag{70}$$

Then,

$$\begin{aligned} Y(s) &= \frac{N}{TR_1} \frac{1 - e^{-sT}}{s + \alpha} \otimes \left[\frac{1 - e^{-sd}}{s} + \frac{(1 - e^{-sd})\, e^{-sT}}{s(1 - e^{-sT})}\right] \\ &= \frac{N(1 - e^{-sT})}{TR_1(s + \alpha)} \left\{1 - e^{-(s+\alpha)d} + \frac{[1 - e^{-(s+\alpha)d}]\, e^{-(s+\alpha)T}}{1 - e^{-(s+\alpha)T}}\right\}. \end{aligned} \tag{71}$$

Since $\alpha d \gg 1$, terms involving the factor $e^{-\alpha d}$ are neglected, and (71) is approximated by

$$Y(s) \cong \frac{N}{TR_1\alpha} (1 - e^{-sT}) \tag{72}$$

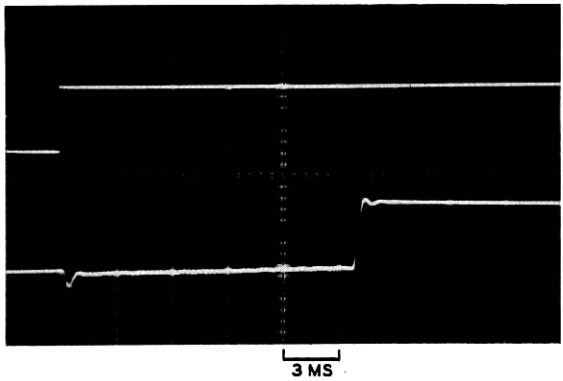

Fig. 9 — Measured step response of delay network.

in the frequency range $| s | \ll \alpha$. Hence, in this limited frequency range the transfer function of the delay network becomes

$$\frac{V_4}{V_1}(s) \cong K - \left(1 + \frac{NR_2}{TR_1\alpha}\right) + \frac{NR_2}{TR_1\alpha} e^{-sT}, \tag{73}$$

which is a constant-delay, all-pass characteristic for

$$K = 1 + \frac{NR_1}{TR_1\alpha} = 1 + \frac{NR_2C}{T}. \tag{74}$$

An exact analysis of the circuit of Fig. 7 indicates that (73) is valid at low frequencies and that, by making the gain of the upper path, K, a frequency-dependent function, the constant-delay characteristic can be obtained over essentially the entire interval $| \omega | < N\omega_0/2$. The measured step response of the delay network is illustrated in Fig. 9. The N-capacitor element was constructed using a 64-contact rotary switch ($d/\tau \cong 0.61$) motor driven at a speed of 60 rps. Capacitors having a value of 0.1 microfarad were connected to each of the contacts.

A useful figure of merit for any delay network is its delay-bandwidth product. In this case, the delay is T seconds. The bandwidth is limited by that of the low-pass filter used to recover the output signal from the sampled data. This bandwidth cannot be greater than $1/2\tau$ cps, and $N\tau = T$, so that

$$\text{(delay) (bandwith)} \cong \frac{N}{2}. \tag{75}$$

5.2 *Narrow-Band Band-Pass Filter*

If the component networks in the N-path sampled-data networks have a low-pass characteristic with bandwidth small compared to ω_0, the transfer function, $F(0,j\omega)$, appears as a sequence of narrow passbands centered at multiples of ω_0, as previously noted. Consequently, this scheme is useful for the realization of highly selective band-pass filters. When only a single passband is required, the realization can be accomplished with a minimum value of $N = 3$, since the transfer function relation is valid for $|\omega| \leqq (N/2)\omega_0$. The band-limiting filter required at the output can also provide a low-frequency cutoff, so that the passband centered at zero frequency can be eliminated; the resulting transfer function is

$$T(j\omega) = \frac{1}{N}\left(\frac{d_1 d_2}{\tau^2}\right)[a_1 H(j\omega - j\omega_0) + a_1^* H(j\omega + j\omega_0)], \quad (76)$$

where

$$a_1 = e^{j(\pi/T)(d_1-d_2)}\left(\frac{\sin\frac{\pi d_1}{T}}{\frac{\pi d_1}{T}}\right)\left(\frac{\sin\frac{\pi d_2}{T}}{\frac{\pi d_2}{T}}\right).$$

This result is similar to the low-pass to band-pass transformation discussed in Section 3.1.

Since the band-pass characteristic is simply a frequency translation of a low-pass characteristic, it has arithmetic symmetry about the center frequency. Another advantage of this realization technique is that the filter can be easily tuned without altering the shape of the characteristic. The tuning is accomplished simply by changing the frequency of the timing source that controls the switching rate.

Implementation of the transfer function of (76) with series-sampling switches would require a current source at the input and negligible loading at the output. Analysis of the more practical circuit of Fig. 10, including source resistance, R_1, and load resistance, R_2, requires a somewhat different approach. Details of this analysis are carried out in Appendix B. The resulting transfer function is again a frequency-translated version of a low-pass characteristic:

$$T(j\omega) = \frac{E_2(j\omega)}{E_1(j\omega)} = \frac{Nd_2}{T}[a_1 G(j\omega - j\omega_0) + a_1^* G(j\omega + j\omega_0)]. \quad (77)$$

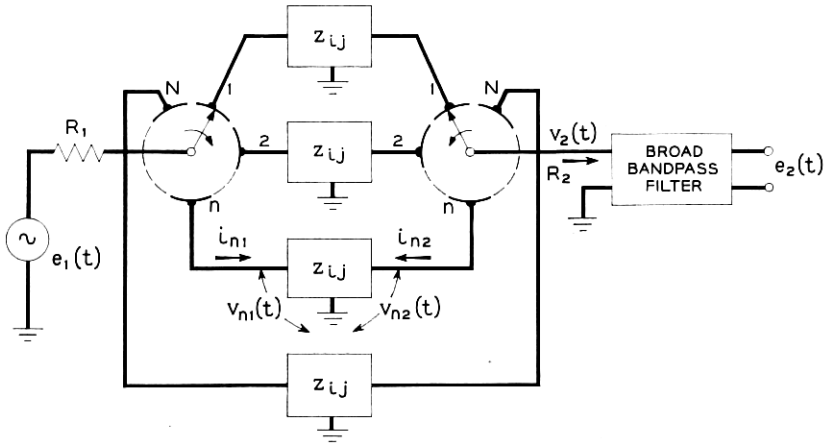

Fig. 10 — Practical circuit for realization of narrow-band filter characteristics.

The low-pass characteristic, $G(j\omega)$, is given by the voltage transfer ratio of one of the component networks operating between a source resistance, R_1T/d_1, and a load resistance, R_2T/d_2, as shown in Fig. 11.

A highly selective narrow-band filter using this scheme with $N = 4$ was constructed, using silicon diode input and output sampling switches controlled by two transistor multivibrator circuits. The center frequency of the filter was set at 25 kc. The low-pass component networks were three-section RC ladder networks with a bandwidth of approximately 3 cps. The Q-factor of a resonant circuit with the same bandwidth and center frequency would be greater than 4000. The selectivity of the sampled-data filter is even greater than the resonant circuit having this Q-factor, since the roll-off rate is greater. The measured frequency-response data and equivalent low-pass network are shown graphically in Fig. 12.

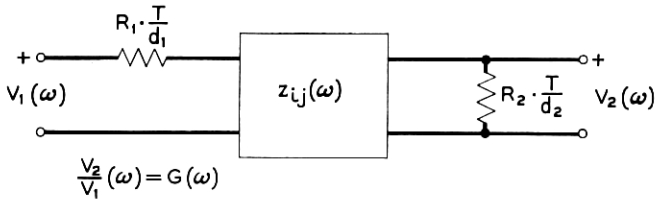

Fig. 11 — Equivalent low-pass network.

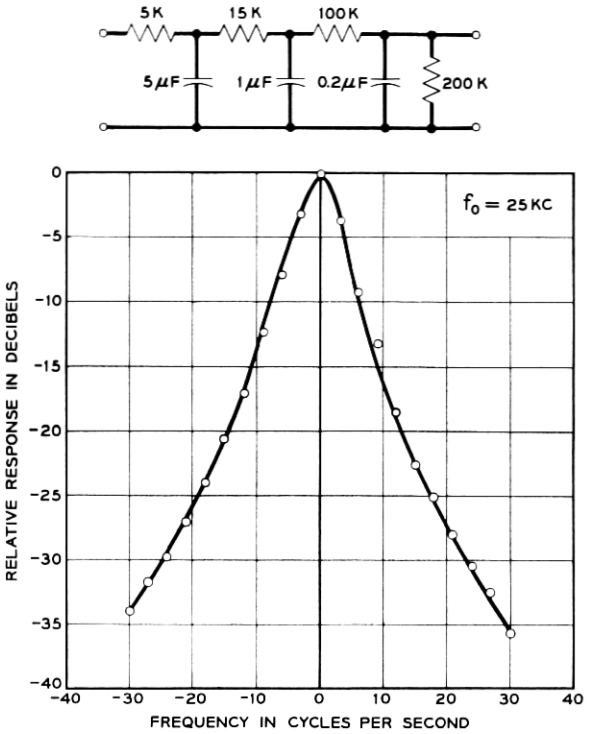

Fig. 12 — Frequency response and one of the constituent equivalent low-pass networks for sampled-data filter.

VI. CONCLUSION

The time-varying network configuration described in this paper exhibits several properties of both theoretical and practical significance.

A general input-output relation for the N-path structure has been derived. With the introduction of band-limiting restrictions, this relation can be expressed by a transfer function that is valid over a frequency band directly proportional to N, the number of parallel paths. In some special cases, however, band-limiting restrictions are unnecessary.

Several useful properties of the transfer function are maintained when the modulation is restricted to a type readily implemented by conventional switching techniques. The case where the modulators are replaced by series-sampling switches is examined in detail.

An important practical feature of the realization techniques discussed

lies in the fact that network characteristics can be controlled by changing the modulation functions rather than by changing circuit element values. Hence, the techniques are readily adaptable to electronic or other automatic methods of control.

APPENDIX A

Determination of the Jump Modulation Function from a Prescribed Set of Fourier Coefficients.

The inversion of (40) could be accomplished by straightforward application of matrix methods, however the particular form of $p(t)$ affords a simple explicit expression for the elements of the inverse matrix. Note that the R functions comprising $p(t)$ in (40) form an orthogonal set, so that

$$\int_0^T p(t)w\left[t - (r-1)\frac{T}{R}\right]dt = \frac{T}{R}p_r. \tag{78}$$

Hence,

$$p_r = \frac{R}{T}\int_0^T \sum_{m=-\infty}^{\infty} P_m e^{j(m2\pi/T)t} w\left[t - (r-1)\frac{T}{R}\right]dt. \tag{79}$$

After interchanging summation and integration (79) becomes

$$\begin{aligned} p_r &= \frac{R}{T}\sum_{m=-\infty}^{\infty} P_m \int_{(r-1)(T/R)}^{r(T/R)} e^{j(m2\pi t/T)}\,dt \\ &= R\sum_{m=-\infty}^{\infty} P_m e^{-j(m\pi/R)}\frac{\sin\dfrac{m\pi}{R}}{m\pi} e^{j(2\pi/R)mr}. \end{aligned} \tag{80}$$

The values of P_m are not independent. From (42), it is seen that

$$P_{m+kR} = \frac{m}{m+kR}P_m. \tag{81}$$

Now (80) can be written as a finite sum over m:

$$p_r = R\sum_{m=-R/2}^{R/2}{}' P_m \frac{e^{-j(m\pi/R)}\sin\dfrac{m\pi}{R}}{\pi} e^{+j(2\pi/R)rm}\sum_{k=-\infty}^{\infty}\frac{m}{(m+kR)^2}, \tag{82}$$

where the prime on the summation over m is taken to mean that when R is even, the end terms of the series ($m = \pm R/2$) are added with half

weight to avoid duplication in the sum over k. The series in k is summable and can be shown to be equal to

$$\sum_{k=-\infty}^{\infty} \frac{m}{(m + kR)^2} = \frac{m\pi^2}{R^2} \csc^2\left(\frac{m\pi}{R}\right). \tag{83}$$

Substitution of (83) into (82) gives

$$p_r = \sum_{m=-R/2}^{R/2}{}' e^{-j(m\pi/R)} \frac{\frac{m\pi}{R}}{\sin \frac{m\pi}{R}} e^{j(2\pi/R)rm} P_m . \tag{84}$$

This expression is written in the two forms of (43) and (44) for the cases of R odd and even respectively.

APPENDIX B

Equivalent Low-Pass Characteristic for Sampled-Data Realization of Band-Pass Filter

Referring to Fig. 10, we see that the following constraints are imposed:

$$\begin{aligned} i_{n1}(t) &= \frac{e_1(t) - v_{n1}(t)}{R_1} p_n(t), \\ i_{n2}(t) &= -\frac{v_{n2}(t)}{R_2} q_n(t); \end{aligned} \tag{85}$$

$$\begin{aligned} I_{n1}(j\omega) = \frac{1}{R_1} \sum_{m=-\infty}^{\infty} P_m e^{-j(m2\pi/T)(n-1)\tau} \\ \cdot [E_1(j\omega - jm\omega_0) - V_{n1}(j\omega - jm\omega_0)], \end{aligned} \tag{86}$$

$$I_{n2}(j\omega) = \frac{1}{R_2} \sum_{m=-\infty}^{\infty} Q_m e^{-j(m2\pi/T)(n-1)\tau} V_{n2}(j\omega - jm\omega_0).$$

Representing the component networks in terms of open-circuit impedance parameters,

$$\begin{aligned} V_{n1}(j\omega) &= z_{11}(j\omega) I_{n1}(j\omega) + z_{12}(j\omega) I_{n2}(j\omega), \\ V_{n2}(j\omega) &= z_{21}(j\omega) I_{n1}(j\omega) + z_{22}(j\omega) I_{n2}(j\omega). \end{aligned} \tag{87}$$

Substitution of (86) into (87) results in infinite-order difference equations in $V_{n1}(j\omega)$ and $V_{n2}(j\omega)$ of the type normally encountered with periodically time-varying networks. However, the fact that the component

networks are designed to have very narrow-band characteristics affords a considerable simplification of the equations.

If

$$| z_{ij}(j\omega) | \cong 0 \qquad \text{for} \quad | \omega | \geqq \frac{\omega_0}{2}, \tag{88}$$

then

$$\begin{matrix} | V_{n1}(j\omega) | \geqq 0 \\ | V_{n2}(j\omega) | \geqq 0 \end{matrix} \qquad \text{for} \quad | \omega | \geqq \frac{\omega_0}{2}. \tag{89}$$

The relations (88) and (89) permit the elimination of all terms except $m = 0$ in the sums involving $V_{n1}(j\omega)$ and $V_{n2}(j\omega)$. Hence, for $| \omega | \leqq \omega_0/2$,

$$\left(1 + \frac{z_{11}}{R_1} P_0\right) V_{n1} + \frac{z_{12}}{R_2} Q_0 V_{n2} = \frac{z_{11}}{R_1} \sum_m P_m e^{-j(m2\pi/T)(n-1)\tau} E_1(j\omega - jm\omega_0), \tag{90}$$

$$\frac{z_{21}}{R_1} P_0 V_{n1} + \left(1 + \frac{z_{22}}{R_2} Q_0\right) V_{n2} = \frac{z_{21}}{R_1} \sum_m P_m e^{-j(m2\pi/T)(n-1)\tau} E_1(j\omega - jm\omega_0), \tag{91}$$

where

$$P_0 = \frac{d_1}{T}, \qquad Q_0 = \frac{d_2}{T}.$$

Eliminating V_{n1} from (90),

$$V_{n2}(j\omega) = \frac{T}{d_1} G(j\omega) \sum_m P_m e^{-j(m2\pi/T)(n-1)\tau} E_1(j\omega - jm\omega_0), \tag{92}$$

where

$$G(j\omega) = \frac{z_{21} R \dfrac{T}{d_2}}{\left(z_{11} + \dfrac{R_1 T}{d_1}\right)\left(z_{22} + \dfrac{R_2 T}{d_2}\right) - z_{12} z_{21}}. \tag{93}$$

The output voltage of the N-path configuration is given by

$$\begin{aligned} v(t) &= \sum_{n=1}^{N} v_n(t) q_n(t), \\ V_2(j\omega) &= \sum_{n=1}^{N} \sum_{l=-\infty}^{\infty} Q_l e^{-j(l2\pi/T)(n-1)\tau} V_{n2}(j\omega - jl\omega_0). \end{aligned} \tag{94}$$

Substituting (92) into (94),

$$\begin{aligned} V_2(j\omega) = \frac{T}{d_1} \sum_{n=1}^{N} \sum_{l,m} Q_l P_m e^{-j[(l+m)2\pi(n-1)/T]\tau} \\ \cdot G(j\omega - jl\omega_0) E_1[j\omega - j(l+m)\omega_0] \end{aligned} \tag{95}$$

and, summing over n as was done in (9),

$$V_2(j\omega) = \frac{NT}{d_1} \sum_{l} Q_l G(j\omega - jl\omega_0) \sum_{k} P_{k-l} E_1(j\omega - jkN\omega_0). \tag{96}$$

Now, if $E_1(j\omega)$ is band-limited such that

$$| E_1(j\omega) | \cong 0 \qquad \text{for} \quad | \omega | \leqq \frac{N\omega_0}{2} \tag{97}$$

and $V_2(j\omega)$ is followed by a low-pass filter with cutoff at $\omega = N\omega_0/2$,

$$\frac{E_2(j\omega)}{E_1(j\omega)} = \frac{NT}{d_1} \sum_{l} Q_l P_{-l} G(j\omega - jl\omega_0). \tag{98}$$

Now, suppose that the low-pass filter is replaced by a band-pass filter that selects only the passband corresponding to $l = \pm 1$. Then,

$$\frac{E_2}{E_1}(j\omega) = \frac{Nd_2}{T} [a_1 G(j\omega - j\omega_0) + a_1^* G(j\omega + j\omega_0)], \tag{99}$$

where

$$a_1 = e^{j(\pi/T)(d_1 - d_2)} \left(\frac{\sin \frac{\pi d_1}{T}}{\frac{\pi d_1}{T}} \right) \left(\frac{\sin \frac{\pi d_2}{T}}{\frac{\pi d_2}{T}} \right).$$

The transfer function of (99) is equivalent to that of (76), where the low-pass function, $G(j\omega)$ in this case, is simply related to the low-pass characteristic of one of the component networks. Examination of the relation (93) shows that $G(j\omega)$ is simply the voltage transfer ratio of one of the component networks operating between a source resistance of $R_1(T/d_1)$ and a load resistance $R_2(T/d_2)$, as shown in Fig. 11. This

equivalent low-pass network provides the basis for synthesis of the prescribed band-pass characteristic.

REFERENCES

1. Paris, H., Utilization of the Quadrature Functions as a Unique Approach to Electronic Filter Design, I.R.E. Conv. Rec., 1960.
2. Linvill, W. K., The Use of Sampled Functions for Time-Domain Synthesis, Proc. Nat. Electronics Conf., Chicago, September 29–30, 1953, Vol. 9, p. 533.
3. LePage, W. R., Cahn, C. R. and Brown, J. S., Analysis of a Comb Filter Using Synchronously Commutated Capacitors, A.I.E.E. Trans., Part I, **72**, 1953, p. 63.
4. Smith, B. D., Analysis of Commutated Networks, I.R.E. Trans., **PGAE-10**, p. 21.